Q-switching instability in a mode-locked semiconductor laser

Dmitrii Rachinskii

Department of Applied Mathematics, University College Cork, Ireland

Andrei Vladimirov and Uwe Bandelow

Weierstrass Institute for Applied Analysis and Stochastics, Mohrenstrasse 39, D-10117 Berlin, Germany

Bernd Hüttl and Ronald Kaiser

Fraunhofer-Institute for Telecommunication, Heinrich-Hertz-Institute, Einsteinufer 37, D-10587, Berlin, Germany

We suggest semianalytic estimates for the *Q*-switching instability boundary of the continuous-wave (cw) mode-locking regime domain for a ring-cavity semiconductor laser. We use a differential delay laser model that allows us to assume large gain and loss in the cavity, which is a typical situation for this class of lasers. The *Q*-switching instability boundary is obtained as a Neimark–Sacker bifurcation curve of a map describing the transformation of pulse parameters after a round trip in the cavity. We study the dependence of this boundary on laser parameters and show that our theoretical results are in qualitative agreement with the experimental data obtained with a passively mode-locked monolithic semiconductor laser. © 2006 Optical Society of America

OCIS codes: 140.4050, 140.5960, 190.3100.

1. INTRODUCTION

Semiconductor lasers operating in the mode-locking (ML) regime are efficient, compact, low-cost sources of short optical pulses with high repetition rates (tens and hundreds of gigahertz) suitable for applications in telecommunication technology. Similarly to other types of lasers, these lasers can be passively mode locked by incorporating a saturable absorber section into the laser cavity. However, apart from ML, lasers with a saturable absorber have a tendency to exhibit undamped *Q*-switching pulsations. In a mode-locked laser the *Q*-switching instability leads to a transition from the cw ML regime to the so-called *Q*-switched ML regime. The latter regime is characterized by pulse amplitude modulated by the *Q*-switching oscillation frequency that is typically on the order of a few gigahertz for semiconductor lasers. Since fluctuations of the ML pulse amplitude are undesirable in most applications, how to avoid this type of instability in real devices is an important question.

Stability of the cw ML regime with respect to the *Q*-switching bifurcation was studied theoretically and experimentally in a number of publications.[1–7] In particular, analytical estimations for the stability criteria for the cw ML regime in a solid-state laser were obtained theoretically under certain approximations.[1,3,5] However, since these studies were based on the Haus master equation, which assumes small gain and loss per cavity round trip and weak saturation of the absorbing medium, their results are hardly applicable in the parameter domain of semiconductor lasers. Therefore, to study ML in these lasers, the approaches based on direct numerical simulations of spatially distributed models are commonly used (for a review see Ref. 8). In this paper we present an alternative approach to describe the *Q*-switching instability in a semiconductor laser, which uses the delay differential model proposed in Ref. 9. Under the slow saturable absorber approximation we derive a map describing the transformation of the ML pulse parameters after a complete round trip in the cavity. A nontrivial fixed point of this map corresponds to a cw ML regime. The *Q*-switching instability threshold is then obtained as a Neimark–Sacker bifurcation of the nontrivial fixed point. We study the dependence of the *Q*-switching instability boundary and the ML stability boundaries obtained by New's criterion[10] on laser parameters and compare them with the results of direct numerical analysis of the original delay differential model. Further modification of our approach, based on the hyperbolic secant ansatz, is used to estimate the width and repetition rate of the ML pulses. Finally, we present some results of the experimental study of a monolithic passively mode-locked semiconductor laser operating at 40 GHz repetition frequency. These experimental data are found to be in qualitative agreement with theoretical results.

2. MODEL EQUATIONS

We consider a ML solution in a model of a semiconductor ring-cavity laser suggested and studied numerically in Ref. 9. In case of the Lorentzian line shape of the spectral filtering element, the model expressed in dimensionless form reads

$$\gamma^{-1}\dot{A} + A = \sqrt{\kappa}e^{[(1-i\alpha_g)G(t-T)/2-(1-i\alpha_q)Q(t-T)/2+i\phi]}A(t-T), \quad (1)$$

$$\dot{G} = g_0 - \gamma_g G - e^{-Q}(e^G - 1)|A|^2, \quad (2)$$

$$\dot{Q} = q_0 - \gamma_q Q - s(1 - e^{-Q})|A|^2, \quad (3)$$

where A is the electric field envelope at the entrance of the absorber section and G and Q stand for saturable gain and loss, respectively. In Eqs. (1)–(3) T is the cold cavity round trip time, the parameter γ measures the bandwidth of the spectral filtering element, κ is the attenuation factor describing linear nonresonant intensity losses per cavity round trip, $\gamma_{g,q}$ are the relaxation rates of the amplifying and absorbing media, s is the ratio of the saturation intensities in gain and absorber media, and ϕ describes the detuning between the central frequency of the spectral filtering element and the nearest cavity mode. The values of dimensionless parameters T, γ^{-1}, and $\gamma_{g,q}^{-1}$ can be converted to real units by multiplication with the time measure unit $\Delta t = 10$ ps. Table 1 represents the parameter set we use in most calculations below.

Equations (1)–(3) give a generalization of Haus' master equation to the case of large gain and loss per cavity round trip, i.e., a situation typical of semiconductor lasers.

Before proceeding to the analysis of a ML regime, we very briefly observe cw solutions of Eqs. (1)–(3) and their Q-switching instability. cw states are defined by the relations $G = G_0$, $Q = Q_0$, $A(t) = A_0 e^{i\gamma\Omega t}$, where $\Omega = \Delta\omega/\gamma$ is the dimensionless frequency shift of the cw solution normalized by the filter bandwidth. Consequently, the constant values of the G and Q components of a cw solution, the amplitude A_0 of the optical field component, and the frequency shift Ω are determined by the system

$$g_0 - \gamma_g G - e^{-Q}(e^G - 1)A_0^2 = 0, \quad q_0 - \gamma_q Q - s(1 - e^{-Q})A_0^2 = 0,$$

$$\kappa e^{G-Q} - 1 - \Omega^2 = 0, \quad (4)$$

and

$$\Omega + \tan[\gamma T\Omega + (\alpha_g G - \alpha_q Q)/2 - \phi] = 0, \quad (5)$$

with the additional condition $\cos[\gamma T\Omega + (\alpha_g G - \alpha_q Q)/2 - \phi] > 0$. As the last equation implies, this system has a countable sequence of solutions (laser modes).

The Q-switching instability corresponds to the Andronov–Hopf bifurcation of the cw solution. If the Q-switching frequency Ω_R and the cw solution frequency shift Ω are much smaller than the ML frequency ($\Omega, \Omega_R \ll \gamma T$), then one arrives at the case of a slowly changing optical field and can neglect the first term $\gamma^{-1}A$ in Eq. (1). Multiplying the resulting equation by its complex conjugate, one gets $P(t+T) = \kappa e^{G(t)-Q(t)}P(t)$, where $P = |A|^2$ is the

Table 1. Parameter Set for Eqs. (1)–(3)

Δt	$T\Delta t$	$\gamma^{-1}\Delta t$	$\gamma_g^{-1}\Delta t$	$\gamma_q^{-1}\Delta t$
10 ps	25 ps	0.2 ps	1 ns	13 ps

k	s	α_g	α_q
0.1	25	0	0

dimensionless optical field power. The assumption of the slowly changing field justifies the further approximation $P(t+T) \approx P(t) + T\dot{P}(t)$, which leads to the approximation of laser equations (1)–(3) by the set of ordinary differential equations

$$T\dot{P} = -P + e^{G-Q+\ln \kappa}P, \quad (6)$$

$$\dot{G} = g_0 - \gamma_g G - e^{-Q}(e^G - 1)P, \quad (7)$$

$$\dot{Q} = q_0 - \gamma_q Q - s(1 - e^{-Q})P. \quad (8)$$

We note that, in the limited case of small G, Q, and $\ln \kappa$, this system transforms to the usual saturable absorber model,[1,11–13] where all exponentials are replaced by their linear approximations. Equations (6)–(8) generalize this simpler model to the case of large gain and loss per cavity round trip.

Although the Q-switching instabilities of the cw and ML solutions are related, we shall see that the Andronov–Hopf bifurcation line of the cw solution of Eqs. (6)–(8) gives only a very rough estimate of the Q-switching instability boundary of the ML regime. The results of numerical calculations are presented below in Section 5 (see Fig. 2).

3. INSTABILITY LEADING TO Q-SWITCHED ML

Now we consider the Q-switching bifurcation of the ML solution. The number of cavity modes that take part in the locking process can be roughly estimated as a ratio of the spectral width γ of the filtering element and the intermode frequency spacing T^{-1}. Here we consider a limit when this number is very large, $\gamma T \to \infty$, which means that the duration τ of a ML pulse is very short, much shorter than the relaxation times of the gain and absorber media, $\tau \ll \gamma_{g,q}^{-1}$. This limit corresponds to the so-called slow saturable absorber approximation,[10,14] which holds quite well for parameter values typical of semiconductor lasers. Analytical study of a ML laser with slow absorber was performed by New[10] and Haus.[14] Following their approach and using the results of Ref. 15, we distinguish between slow and fast stages in the evolution of a ML solution. The fast stage corresponds to a short time interval during which the amplitude of the pulse is large. During this stage linear relaxation terms in the right-hand side of Eqs. (2) and (3) can be neglected. The slow stage corresponds to the time interval during which the electric field intensity is small between two subsequent pulses. At this stage we neglect the terms proportional to $|A|^2$ in the right-hand side of Eqs. (2) and (3). Solving the laser equations for the two stages separately and then combining the solutions, we obtain a map that describes the transformation of pulse parameters after a complete round trip in the cavity. A fixed-point solution of this map corresponds to a ML solution characterized by the periodic laser intensity. We study the stability of the fixed point and demonstrate that it can exhibit a Neimark–Sacker bifurcation characterized by a pair of complex conjugate Flo-

quet multipliers crossing the unit cycle. This bifurcation is responsible for a Q-switching instability of the ML regime.

Let G_n and Q_n be the saturable gain and loss evaluated at the beginning of the fast stage after n round trips in the cavity, i.e., at the leading edge of the nth pulse. The corresponding pulse energy is given by $P_n = \int_0^{\tau_n} |A|^2 dt$, where the integration limits, 0 and τ_n, stand for the beginning and end of the nth fast stage, respectively. During the fast stage the laser intensity is large, and the terms containing $|A|^2$ become dominant in Eqs. (2) and (3). Thus we neglect the other (relaxation) terms in the right-hand side of these equations to arrive at the system $\dot{G} = -e^{-Q}(e^G - 1)|A|^2$ and $\dot{Q} = -s(1 - e^{-Q})|A|^2$, which admits the explicit solution

$$G(p) = -\ln\left[1 - \frac{1 - e^{-G_n}}{(1 + e^{sp - Q_n} - e^{-Q_n})^{1/s}}\right],$$

$$Q(p) = \ln[1 + e^{-sp}(e^{Q_n} - 1)], \qquad (9)$$

where p is the differential energy of the nth pulse defined by $dp = |A|^2 dt$. The slow stage of a ML solution is described by the linear ordinary differential equations, $\dot{Q} = q_0 - \gamma_q Q$ and $\dot{G} = g_0 - \gamma_g G$, with the solutions

$$G(t) = G(P_n)e^{-\gamma_g t} + \frac{g_0}{\gamma_g}(1 - e^{-\gamma_g t}),$$

$$Q(t) = Q(P_n)e^{-\gamma_q t} + \frac{q_0}{\gamma_q}(1 - e^{-\gamma_q t}), \qquad (10)$$

where the initial conditions, $G(P_n)$ and $Q(P_n)$, are obtained from Eqs. (9) with $p = P_n$. Substituting Eqs. (9) into Eqs. (10) and taking into account that in the limit $\gamma T \to \infty$ the duration of the slow stage is equal to the cavity round trip time T, we obtain a map describing the transformation of the saturable gain and loss after a complete round trip in the cavity:

$$G_{n+1} = -e^{-\gamma_g T}\ln\left[1 - \frac{1 - e^{-G_n}}{(1 + e^{sP_n - Q_n} - e^{-Q_n})^{1/s}}\right] + (1 - e^{-\gamma_g T})g_0/\gamma_g, \qquad (11)$$

$$Q_{n+1} = e^{-\gamma_q T}\ln[1 + e^{-sP_n}(e^{Q_n} - 1)] + (1 - e^{-\gamma_q T})q_0/\gamma_q. \qquad (12)$$

Here G_{n+1} and Q_{n+1} are the saturable gain and loss evaluated at the beginning of the fast stage after $n + 1$ round trips in the cavity, i.e., at the leading edge of the $(n+1)$th pulse.

To complete Eqs. (11) and (12) one must relate the energies P_n and P_{n+1} of two subsequent pulses by solving Eq. (1) for the electric field envelope A. Unfortunately, this task cannot be performed analytically in a general situation. Therefore we use two different approaches to simplify the problem. The first of them is based on New's approximation,[10] which assumes that there is no spectral filtering in the cavity. This approach allows for the calculation of the Q-switching instability boundary of a ML so-

lution and background stability boundaries of a ML pulse according to the criterion proposed by New.[10] However, such important characteristics of the ML regime as pulse duration and deviation of the pulse repetition period from the cold cavity round-trip time are missing in this approach. Therefore, in order to get these characteristics, in Section 5 we apply a variational approach to a more realistic situation when spectral filtering is taken into account.

4. NO SPECTRAL FILTERING IN THE CAVITY

Let us rewrite Eq. (1) equivalently in the form

$$\gamma^{-1}\dot{A}_{n+1}(t - \gamma^{-1}\delta_n) + A_{n+1}(t - \gamma^{-1}\delta_n)$$
$$= \sqrt{\kappa}e^{\left[\frac{1 - i\alpha_g}{2}G(t) - \frac{1 - i\alpha_q}{2}Q(t)\right]}A_n(t). \qquad (13)$$

In Eq. (13) $A_{n+1}(t) \equiv A_n(t + T_n)$ and $\delta_n = \gamma(T_n - T)$, where T_n is the time interval between the two subsequent pulses. Multiplying Eq. (13) with its conjugate and integrating over the round trip time T we get

$$\gamma^{-2}\int_0^{\tau_{n+1}} |\dot{A}_{n+1}|^2 dt + P_{n+1} = \kappa \int_0^{P_n} e^{G(p) - Q(p)} dp, \qquad (14)$$

where in both sides we have restricted the integration to the fast stage since the optical field intensity during the slow stage is negligibly small. Equation (14) describes the energy balance in the cavity. It is similar to Eq. (46) in Ref. 14, which was derived for a periodic ML solution under small gain and loss per cavity round trip and parabolic dispersion approximations, and to a generalization of this equation in the case of large gain and loss obtained in Ref. 15. The integral term in the left-hand side of Eq. (14) describes energy losses introduced by the spectral filtering element. Since in this section we neglect the spectral filtering completely, this term can be dropped. Then, after explicit integration of the right hand side we obtain

$$P_{n+1} = \kappa \ln[1 - e^{G_n} + e^{G_n}(1 + e^{sP_n - Q_n} - e^{-Q_n})^{1/s}]. \qquad (15)$$

The three-dimensional map [Eqs. (11), (12), and (15)] describes the transformation of the pulse parameters G_n, Q_n, and P_n after a complete round trip in the cavity. It always has a trivial fixed point $(g_0/\gamma_g, q_0/\gamma_q, 0)$ corresponding to zero pulse power (i.e., to laser-off). This point is stable for $\eta = g_0/\gamma_g - q_0/\gamma_q + \ln \kappa < 0$ and loses stability via a transcritical bifurcation at the linear laser threshold $\eta = 0$. A fixed point (G_*, Q_*, P_*) with $P_* > 0$ that appears after the transcritical bifurcation represents a pulsed solution of Eqs. (1)–(3) with the periodic laser intensity corresponding to a fundamental ML regime. Depending on the parameter values, the fixed point characterized by a positive pulse energy can bifurcate from the trivial one, either supercritically or subcritically. In the latter case there may be a bistability between the zero intensity solution and the solution corresponding to a ML regime. In this paper, however, we consider only the parameter values satisfying the inequality

$$(\kappa^{-1} - e^{-q_0/\gamma_q})\tanh\frac{\gamma_q T}{2} > s(1 - e^{-q_0/\gamma_q})\tanh\frac{\gamma_g T}{2}, \quad (16)$$

which implies that the stable fixed point (G_*, Q_*, P_*) with $P_* > 0$ bifurcates from the trivial one supercritically, whereby bistability is excluded.

We have observed numerically by the linear stability analysis that the fixed point (G_*, Q_*, P_*) can lose stability via the so-called Neimark–Sacker bifurcation where two complex conjugated Floquet multipliers cross the unit circle. This bifurcation is similar to the Andronov–Hopf bifurcation of ordinary differential equations. A solution that appears at the bifurcation point corresponds to a regime with ML pulse energy modulated periodically at the Q-switching frequency. The Neimark–Sacker bifurcation curve QS shown in Fig. 1 by a solid curve represents the border between the ML and Q-switching domains in the parameter plane $(g_0, -q_0)$. The fixed point (G_*, Q_*, P_*) exists to the right from the linear threshold line th and is stable in the area above the curve QS.

Another stability criterion of ML solution was proposed by New.[10] According to this criterion, ML pulses are stable if the net gain parameter $G(t) - Q(t) + \ln\kappa$ is negative during the whole slow stage. Physically this means that small perturbations of the low intensity background between two subsequent pulses do not grow with time. Though stable ML pulses that do not satisfy New's criterion were observed in numerical simulations,[4,6,9] these pulses are expected to be very sensitive to the presence of noise. Therefore one can expect that this criterion gives at least a rough estimation of the ML stability domain.

As one can see from Eq. (10), New's background stability criterion is fulfilled if the net gain is negative at the beginning and the end of the slow stage. Therefore the boundaries of the background stability domain of ML pulses are defined by the equalities

$$G_* - Q_* + \ln\kappa = 0, \quad \widetilde{G}_* - \widetilde{Q}_* + \ln\kappa = 0. \quad (17)$$

Here $\widetilde{G}_* = G(P_*)$ and $\widetilde{Q}_* = Q(P_*)$, defined by Eq. (9), describe the saturable gain and loss at the beginning of the slow stage. They are obtained from Eqs. (9) by the substitution $Q_n \rightarrow Q_*$, $G_n \rightarrow G_*$, and $p \rightarrow P_*$. Eqs. (17) defines the leading and the trailing edge instability boundaries of a ML pulse in the laser parameter space. These boundaries are shown in Fig. 1 by the solid curves L and T, respectively. One can see that the lower boundary T of the background stability domain is separated from the bifurcation boundary QS by a thin stripe, where ML pulses with unstable background are stable with respect to the Q-switching instability. The existence of stable ML pulses with unstable background, according to New's criterion, was noticed in numerical simulations using both the Haus master equation[4,6] and the delay differential model [Eqs. (1)–(3)].[9,16] The two background instability boundaries L and T meet each other at the codimension-two point CT. The coordinates of this point, which lie at the linear threshold line th and, therefore, correspond to infinitely small pulse energy, can be expressed explicitly: $g_0 = \gamma_g \ln[(s-1)/(s\kappa-1)]$, $q_0 = \gamma_q \ln[\kappa(s-1)/(s\kappa-1)]$; see Ref. 15. The circles in Fig. 1 represent the points at the Q-switching (empty circles) and background (full circles)
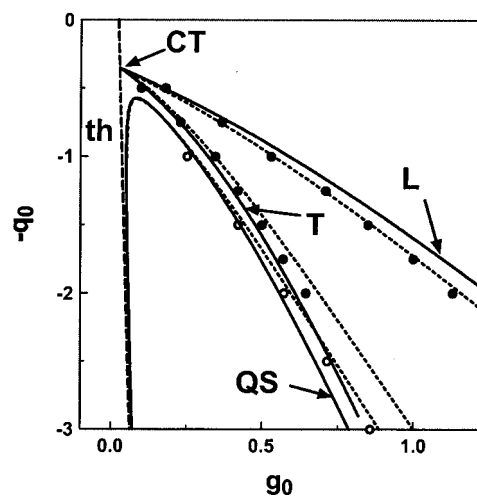

Fig. 1. Q-switching instability curves (QS) and background instability boundaries (L and T) of a ML pulse. L, leading-edge; T, trailing-edge instability boundary. Solid curves are obtained using Eqs. (11), (12), and (15). Dashed curves are obtained from Eqs. (11), (12), (19), and (20). Dots show Q-switching and background instability boundaries calculated by direct numerical integration of the laser equations (1)–(3). The straight line th indicates the linear lasing threshold. Parameters are as in Table 1.
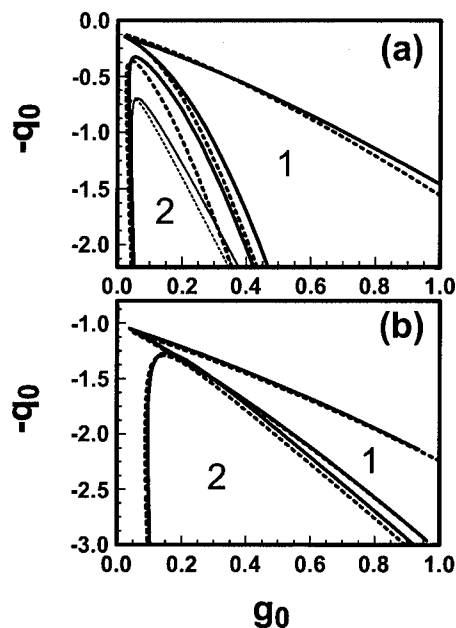

Fig. 2. Background stability 1 and ML Q-switching instability 2 domains. (a) $s\kappa = 5$ and (b) $s\kappa = 1.3$. Solid and dashed curves present the Q-switching and background instability boundaries of the ML solution calculated for $s = 35$ and $s = 15$, respectively. Thin curves in (a) indicate the Q-switching instability of the cw regime. This latter instability does not exist for $s\kappa = 1.3$. Other parameters are the same as in Fig. 1.

instability boundaries obtained by means of direct numerical simulation of Eqs. (1)–(3). One can see that these numerical results are in quite good agreement with those obtained analytically in the limit when the spectral filtering is neglected.

Figure 2 presents the dependence of the ML Q-switching and background instability boundaries on the linear loss parameter κ and the ratio s of the satura-

tion intensities in gain and absorbing media. The boundaries shown by thick solid and dotted curves have been calculated using Eqs. (11), (12), (15), and (17). It follows from our numerical simulations that these boundaries depend mainly on the product $s\kappa$ and weakly depend on these two parameters separately. This property holds especially well for large cavity losses typical for semiconductor lasers, as illustrated by Fig. 2. According to this figure, the domain of the Q-switched ML regime is shifted into the region of large linear gain g_0 and linear loss q_0 parameters and becomes wider with the decrease of $s\kappa$. This is in agreement with the experimental observations of Ref. 2, where it was shown that the ML stability domain of a monolithic semiconductor laser can be enlarged by increasing the laser facets reflectivity. Thin curves in Fig. 2(a) indicate the Q-switching instability boundaries of the cw state calculated at $s\kappa=5$ using Eqs. (6)–(8) (the thin solid curve corresponds to $s=35$; the thin dotted curve corresponds to $s=15$). For these parameter values the Q-switching bifurcations of the cw and ML solutions are not far away from one another. However, for the parameter values of Fig. 2(b) ($s\kappa=1.3$), the Andronov–Hopf bifurcation of the cw solution disappears and hence cannot be used to estimate the Q-switching threshold of the ML regime anymore.

On a qualitative level, the effect of the parameters s and κ on the properties of a mode-locked laser allows simple explanation. The ratio s of the saturation energies of the two laser sections is associated with the main nonlinear mechanism responsible for the compression of the ML pulse. Therefore one can expect an improvement of ML quality and a decrease of the pulse width with the increase of this parameter. According to Eqs. (1)–(3), the attenuation factor κ describes the round-trip feedback strength that is also responsible for one of the main mechanisms of the formation of the ML pulse. In the case when κ is too small, the amplitude of the pulse returning to the absorber section after a round trip in the cavity is not sufficient to create a net gain window necessary to maintain the ML regime. Thus one also expects that the increase of κ must be helpful for ML. Below in Section 6 we present some experimental confirmation of these qualitative conclusions. Of course, the results of our quantitative method and quantitative conclusions like that the product $s\kappa$ are that the main parameter lies beyond the scope of this simple qualitative argumentation.

5. VARIATIONAL APPROACH
The reduced model [Eqs. (11), (12), and (15)] is based on the representation of a ML solution by the T-periodic sequence of δ pulses with the energy P_*. Note that this map does not depend on the α factors $\alpha_{g,q}$. Also, it gives no information about such important characteristics of the ML regime as the pulse width and deviation of the pulse repetition period from the cold cavity round-trip time T. To estimate these characteristics, we modify our map using a variational approach. We look for the solution of Eq. (1) at the nth fast stage in the form

$$A_n(t) = \sqrt{\frac{P_n \gamma}{2\tau_n}}\, \text{sech}\left(\frac{\gamma t}{\tau_n}\right), \qquad (18)$$

where P_n is the dimensionless pulse energy and τ_n/γ is the pulse width. In doing so, we are motivated by the fact that Haus' formula [Eq. (18)] (see Ref. 14) gives an exact solution of the ML problem in the weak saturation limit when all the nonlinearities can be replaced by their second-order Taylor expansions in the pulse energy P.

For simplicity, we consider the case of zero α factors, consequently $\alpha_g = \alpha_q = 0$. Substituting Eq. (18) into Eq. (14) and taking into account that the right-hand side of this equation is equal to the right-hand side of Eq. (15), we obtain

$$\frac{P_{n+1}}{3\tau_{n+1}^2} + P_{n+1} = \kappa \ln[1 - e^{G_n} + e^{G_n}(1 + e^{sP_n - Q_n} - e^{-Q_n})^{1/s}].$$

$$(19)$$

It is important to note that since in the limit of infinite bandwidth, $\gamma T \to \infty$, the normalized pulse width τ remains finite, both the terms in the left-hand side of Eq. (19) are of the same order, while in New's approach the first term was neglected. It means that Eq. (19) obtained for the Lorentzian filtering in the limit of infinitely broad bandwidth $\gamma T \to \infty$ and Eq. (15) based on New's assumption that spectral filtering is absent lead to different estimates of the ML pulse energy.

Thus, in the presence of spectral filtering, we replace Eq. (15) by Eq. (19), while Eqs. (11) and (12), which do not depend on the pulse shape, remain unchanged. Since Eq. (19) contains an additional parameter, the normalized pulse width τ_n, an extra relation is required to describe the evolution of this parameter from one pulse to another. We obtain it by integrating Eq. (13) over the cavity round-trip time, which seems to be a reasonable and simple possibility among the others (leading to different relations). We neglect the optical field intensity during the slow stage and then integrate Eq. (13) with G, Q, A_n, and A_{n+1} replaced by the corresponding fast stage solutions of Eqs. (9) and (18), and $A_{n+1}(t) = [\gamma P_{n+1}/(2\tau_{n+1})]^{1/2}\text{sech}(\gamma t/\tau_{n+1})$. Taking the square of both sides of the resulting equation, in the limit $\gamma T \to \infty$ we arrive at

$$\tau_{n+1} P_{n+1} = \kappa \tau_n P_n \left[\frac{1}{\pi} \int_0^{P_n} \frac{\Phi(p, Q_n, G_n)}{\sqrt{p(P_n - p)}}\, dp \right]^2, \qquad (20)$$

with

$$\Phi(p, Q_n, G_n) = [1 + e^{-sp}(e^{Q_n} - 1)]^{-1/2}$$

$$\times \left[1 - \frac{1 - e^{-G_n}}{(1 + e^{sp - Q_n} - e^{-Q_n})^{1/s}} \right]^{-1/2}. \qquad (21)$$

We analyze the four-dimensional map [Eqs. (11), (12), (19), and (20)] in the same way as the three-dimensional one of Section 4, again interpreting a stable fixed point (G_*, Q_*, P_*, T_*) with a positive pulse energy P_* as a representation of the fundamental ML solution and the Neimark–Sacker bifurcation line as the border between the Q-switching and ML domains. Figure 1 allows us to compare this border and the region of stability of ML

pulses background obtained for the four-dimensional model (dashed curves) with that of the three-dimensional model (solid curves) and with the results of numerical analysis of the complete model [Eqs. (1)–(3)] (shown by circles). One can see that, as it might be expected, the results obtained with the four-dimensional map appear to be in better agreement with the results of direct numerical simulations of the delay differential equations. However, the discrepancy between the stability boundaries obtained with and without spectral filtering is not so pronounced for the parameter values of Fig. 1. A more important advantage of the approach based on the four-dimensional map is that it allows us to estimate the normalized pulse width τ_* and the normalized difference $\delta_* = \gamma(T_* - T)$ between the pulse repetition period and the cavity round-trip time. The first of these two quantities is obtained by calculating the fourth component of the nontrivial fixed point of the map [Eqs. (11), (12), (19), and (20)]. The second quantity can be obtained similarly to the derivation of Eq. (20) above. For a T_*-periodic ML solution, Eq. (13) becomes

$$\gamma^{-1}\dot{A}(t - \gamma^{-1}\delta_*) + A(t - \gamma^{-1}\delta_*) = \sqrt{\kappa}e^{[G(t)-Q(t)]/2}A(t). \quad (22)$$

Substituting fast-stage solutions (9) and (18) into this equation, multiplying it by t, and integrating over the round-trip time, we arrive at the formula

$$\delta_* = 1 + \frac{\tau_*\sqrt{\kappa}}{\pi}\int_0^{P_*}\frac{\Phi(p,Q_*,G_*)}{\sqrt{p(P_*-p)}}\operatorname{arctanh}\left(\frac{2p}{P_*}-1\right)\mathrm{d}p,$$

$$(23)$$

where (Q_*,G_*,P_*,r_*) is the fixed point of the map (11), (12), (19), and (20). Figures 3(a) and 3(b) show how the quantities τ_* and δ_* change along the boundaries of the background stability domain. We have found that, similarly to the background and Q-switching instability do-
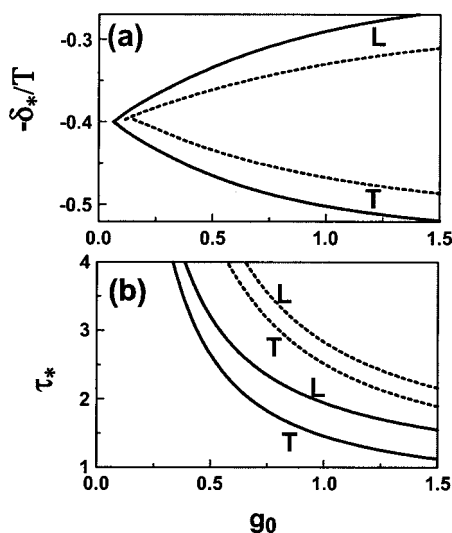

Fig. 3. (a) Normalized difference between the ML pulse repetition period T_* and the cavity round-trip time T. (b) Normalized width τ_* of a ML pulse. Curves L (T) correspond to the leading (trailing) edge instability boundaries shown in Fig. 1. Solid and dotted curves correspond to $s\kappa=5$ and $s\kappa=1.3$, respectively. Other parameters are the same as in Fig. 1.

main boundaries shown in Fig. 2, these two quantities depend very weakly on the parameters s and κ separately in the case when the product $s\kappa$ is fixed. Therefore in each plot of Fig. 3 the results obtained with two different values of the product $s\kappa$ are presented. The curves labeled L and T correspond, respectively, to the leading and trailing edge instability boundaries. It follows from Fig. 3(b) that the pulse width is smaller at the trailing edge instability boundary, which is close to the Q-switching curve QS. With the increase of the product $s\kappa$ the pulse width decreases. Both these results are in qualitative agreement with the experimental data presented in the next section. The quantity $-\delta_*$ increases (decreases) with the increase of the pump parameter at the curves L (T). This means that the pulse repetition rate increases with g_0 at the leading-edge instability boundary and decreases at the trailing-edge instability boundary. The reason is that the net gain window is shifted near the boundary L to the leading edge of a pulse and, hence, the ML pulse is accelerated by the nonlinear intracavity media. Similarly, near the trailing-edge instability boundary pulses are delayed by a net gain window, which is shifted to their trailing edge in this case. The point where the two curves, L and T, meet each other in Fig. 3(a) lies on the linear threshold and corresponds to infinitely small pulse energy. At this point the quantity $-\delta_*$ is negative owing to the dispersion introduced by the spectral filtering element.

6. COMPARISON WITH EXPERIMENTAL RESULTS

The experiments were performed with a monolithic passively mode-locked semiconductor laser comprising four sections: saturable absorber, gain, phase tuning, and a distributed Bragg reflector section, which is responsible for the spectral filtering of laser radiation. The phase shift and losses introduced by the phase tuning section can be controlled by the current applied to this section. More details concerning the experimental device can be found in Ref. 17. The gray shaded areas in Fig. 4 present the experimentally measured ML regimes with the repetition frequency close to 40 GHz obtained for different values of the phase section current. In this figure, different pulse widths are indicated by different levels of gray color. In white regions below the gray ML domains and above the generation threshold, the laser exhibits Q-switched ML regimes. Figure 4(a), corresponding to smaller cavity losses (phase current is equal to zero), demonstrates a larger ML domain and a smaller Q-switching domain, which is in qualitative agreement with the theoretical results shown in Fig. 2. We note that this is also in agreement with the experimental results reported earlier.[2] In addition, the ML area in Fig. 4(b) is slightly down-shifted with respect to that in Fig. 4(a). Similar behavior is observed in Fig. 2.

According to our theoretical results, the effect of the increase of the parameter κ (decrease of the cavity losses) is similar to that of the increase of the ratio s of the saturation energies of the gain and absorber sections. Unfortunately, one can hardly change this latter parameter in the same device. Therefore in Fig. 5 we present the results of
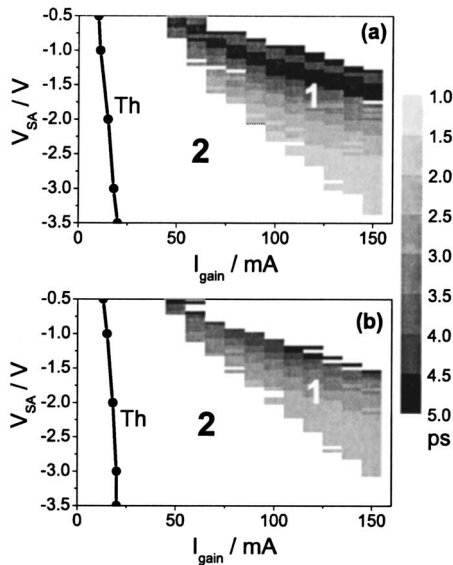
Fig. 4. Experimentally measured ML domain 1. Different pulse widths are shown by different depth of the gray color. In the white area 2 below the ML domains and above the threshold line indicated Th the Q-switched ML regimes have been observed. (a) Laser with normal losses. (b) Laser with extra losses introduced by applying additional current to the passive section.
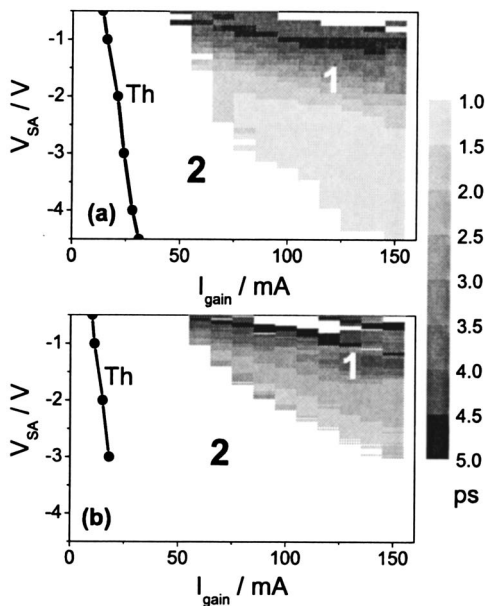

Fig. 5. The same as Fig. 4 but for two lasers with different number of quantum wells in both gain and absorber sections. (a) A laser with three quantum wells; (b) a laser with six quantum wells. The ML area is much larger for the three quantum-well laser than for the six quantum-well one.

the experimental study of two lasers characterized by a different number of quantum wells in both absorber and gain sections. Figure 5(a), corresponding to the laser with three quantum wells, exhibits a larger ML area and smaller pulse widths than Figure 5(b) obtained for the six quantum-well laser. This could be qualitatively explained by the increase of the saturation energies ratio s in a laser with smaller number of quantum wells. As was shown in Ref. 17, the laser with three quantum wells is character-

ized by much smaller differential gain parameter and hence much larger saturation gain energy than that with six quantum wells.

7. CONCLUSION

In this paper, using a slow saturable absorber approximation, we described the Q-switching instability in a mode-locked semiconductor laser. We constructed an analytical map that describes the transformation of ML pulse parameters after a complete round trip in the cavity. The Q-switching instability boundary was found as a Neimark–Sacker bifurcation of this map. According to our results, this boundary can be quite well estimated by the approach of New that neglects spectral filtering. To determine the pulse width and repetition frequency, we have applied a more advanced approach based on variational techniques. We have shown that the Q-switching instability boundary depends strongly on the product of the stability parameter s and the linear nonresonant loss parameter κ is weakly dependent on each of these two parameters separately if $s\kappa$ is fixed. Our estimations of the dependence of the Q-switching instability and the ML stability domains on the laser parameters are in qualitative agreement with experimental data obtained with a monolithic mode-locked semiconductor laser.

ACKNOWLEDGMENTS

REFERENCES

1. H. A. Haus, "Parameter ranges for cw passive mode locking," IEEE J. Quantum Electron. **12**, 169–176 (1976).
2. J. Palaski and K. Lau, "Parameter ranges for ultrahigh frequency mode locking of semiconductor lasers," Appl. Phys. Lett. **59**, 7–9 (1991).
3. F. Kärtner, L. Brovelli, D. Kopf, M. Kamp, I. Calasso, and U. Keller, "Control of solid-state laser dynamics by semiconductor devices," Opt. Eng. **34**, 2024–2036 (1995).
4. J. L. A. Dubbeldam, J. A. Leegwater, and D. Lenstra, "Theory of mode-locked semi-conductor lasers with finite relaxation times," Appl. Phys. Lett. **70**, 1938–1940 (1997).
5. C. Hönniger, R. Paschotta, F. Morier-Genoud, M. Moser, and U. Keller, "Q-switching stability limits of continuous-wave passive mode locking," J. Opt. Soc. Am. B **16**, 46–56 (1999).
6. R. Paschotta and U. Keller, "Passive mode-locking with slow saturable absorbers," Appl. Phys. B **73**, 653–662 (2001).
7. T. Kolokolnikov, Department of Mathematics and Statistics, Dalhousie University, Halifax, Nova Scotia, Canada B3H 3J5; T. Erneux, Optique Nonlinéaire Théorique, Université Libre de Bruxelles, Campus Plaine CP 231, B-1050 Bruxelles, Belgium; N. Joly, Department of Physics, Centre for Photonics and Photonic Materials, University of Bath, Bath BA2 7AY, United Kingdom;

and S. Bielawski, Laboratoire de Physique des Lasers, Atomes et Molécules, UMR CNRS 8523, Centre d'Études et de Recherches Lasers et Applications, FR CNRS 2416, Université des Sciences et Technologies de Lille, F-59655 Villeneuve D'Ascq Cedex, France, are preparing a manuscript titled, "The Q-switching instability in passively mode-locked lasers."

8. E. Avrutin, J. Marsh, and E. Portnoi, "Monolithic and multi-GigaHertz mode-locked semiconductor lasers: constructions, experiments, models, and applications," IEE Proc.: Optoelectron. **147**, 251–278 (2000).

9. A. Vladimirov, D. Turaev, and G. Kozyreff, "Delay differential equations for mode-locked semiconductor lasers," Opt. Lett. **29**, 1221–1223 (2004).

10. G. H. C. New, "Pulse evolution in mode-locked quasi-continuous lasers," IEEE J. Quantum Electron. **10**, 115–124 (1974).

11. P. Mandel and T. Erneux, "Stationary, harmonic, and pulsed operations of an optically bistable laser with saturable absorber: I," Phys. Rev. A **30**, 1893–1901 (1984).

12. T. Erneux, "Q-switching bifurcation in a laser with a saturable absorber," J. Opt. Soc. Am. B **5**, 1063–l069 (1988).

13. M. Yamada, "A theoretical analysis of self-sustained pulsation phenomena in narrow-stripe semiconductor lasers," IEEE J. Quantum Electron. **QE-29**, 1330–1336 (1993).

14. H. Haus, "Theory of mode locking with a slow saturable absorber," IEEE J. Quantum Electron. **11**, 736–746 (1975).

15. A. Vladimirov and D. Turaev, "Model for passive mode-locking in semiconductor lasers," Phys. Rev. A **72**, 033808 (2005).

16. A. Vladimirov and D. Turaev, "A new model for a mode-locked semiconductor laser," Radiophys. Quantum Electron. **47**, 857–865 (2004).

17. B. Hüttl, R. Kaiser, W. Rehbein, H. Stolpe, C. Kindel, S. Fidorra, A. Steffan, A. Umbach, and H. Heidrich, "Low noise monolithic 40 GHz mode-locked DBR lasers based on GaInAsP/InP," presented at the 17th Indium Phosphide and Related Materials Conference, Glasgow, UK, 8–12 May 2005.